Nuclear Engineering and Technology 52 (2020) 621–625

Contents lists available at ScienceDirect

Nuclear Engineering and Technology

journal homepage: www.elsevier.com/locate/net

Original Article

Applicability of nonlinear ultrasonic technique to evaluation of thermally aged CF8M cast stainless steel

Jongbeom Kim [a], Jin-Gyum Kim [b], Byeongseo Kong [c], Kyung-Mo Kim [a], Changheui Jang [c], Sung-Sik Kang [b, *], Kyung-Young Jhang [d, **]

[a] Korea Atomic Energy Research Institute, Daejeon, 34057, Republic of Korea
[b] Korea Institute of Nuclear Safety, Daejeon, 34142, Republic of Korea
[c] Department of Nuclear and Quantum Engineering, Korea Advanced Institute of Science and Technology, Daejeon, 34141, Republic of Korea
[d] School of Mechanical Engineering, Hanyang University, Seoul, 04736, Republic of Korea

ARTICLE INFO

Article history:
Received 10 July 2019
Received in revised form
29 August 2019
Accepted 10 September 2019
Available online 12 September 2019

Keywords:
Cast austenitic stainless steel
CF8M
Nonlinear ultrasonic technique
Tensile test

ABSTRACT

Cast austenitic stainless steel (CASS) is used for fabricating different components of the primary reactor coolant system of pressurized water reactors. However, the thermal embrittlement of CASS resulting from long-term operation causes structural safety problems. Ultrasonic testing for flaw detection has been used to assess the thermal embrittlement of CASS; however, the high scattering and attenuation of the ultrasonic wave propagating through CASS make it difficult to accurately quantify the flaw size. In this paper, we present a different approach for evaluating the thermal embrittlement of CASS by assessing changes in the material properties of CASS using a nonlinear ultrasonic technique, which is a potential nondestructive method. For the evaluation, we prepared CF8M specimens that were thermally aged under four different heating conditions. Nonlinear ultrasonic measurements were performed using a contact piezoelectric method to obtain the relative ultrasonic nonlinearity parameter, and a mini-sized tensile test was performed to investigate the correlation of the parameter with material properties. Experimental results showed that the ultrasonic nonlinearity parameter had a correlation with tensile properties such as the tensile strength and elongation. Consequently, we could confirm the applicability of the nonlinear ultrasonic technique to the evaluation of the thermal embrittlement of CASS.

1. Introduction

Cast austenitic stainless steel (CASS) is used for fabricating different components of the primary reactor coolant system of pressurized water reactors (PWRs), such as reactor coolant pumps, pipes, and valves because of its good weldability, high strength, and high corrosion resistance [1]. However, CASS has the drawback that it is susceptible to thermal embrittlement caused by the cleavage of the ferrite phase or the precipitation of carbides between the ferrite and austenite phase boundaries. Therefore, the thermal embrittlement resulting from the long-term operation of PWRs causes the loss of the fracture toughness of CASS [2].

The Generic Aging Lessons Learned Report (section XI.M12) of the U.S. NRC [3], which is a reference document for the evaluation of the degradation of long-term-operating nuclear power plants, suggests that nondestructive testing such as enhanced visual testing and ultrasonic testing (UT) should be performed as an indirect method to assess the reduction in the fracture toughness of CASS caused by thermal embrittlement. However, it is difficult to obtain the reliability of UT for flaw detection because the ultrasonic wave propagating through CASS is scattered and attenuated by coarse particles and anisotropic microstructures [4–7]. Therefore, the nondestructive testing of CASS using UT remains a major challenge. To overcome this limitation, many researchers have attempted to establish guidelines for flaw detection using UT.

Anderson et al. assessed the usefulness of low-frequency UT for the detection of inner surface-breaking cracks in CASS piping weldments by applying the phased-array ultrasonic technique (PAUT) [7] because low-frequency UT offers the capability of penetrating the thick walls of primary piping circuits. Their results indicated that the low-frequency PAUT could be used to estimate

* Corresponding author.
** Corresponding author.
E-mail addresses: sskang@kins.re.kr (S.-S. Kang), kyjhang@hanyang.ac.kr (K.-Y. Jhang).

https://doi.org/10.1016/j.net.2019.09.004

the length of rough cracks; however, the root-mean-square error value for the obtained results did not satisfy the American Society of Mechanical Engineers (ASME) Boiler & Pressure Vessel Code (BPVC) Section XI [8]. Jacob et al. performed a round-robin test to establish the inspection guidelines because the ASME BPVC Section XI [8] does not specify the inspection procedure and guidelines for CASS [9]. The round-robin test results indicated that the PAUT performed using a 500-kHz ultrasonic wave was the most effective method to examine CASS pipes with diameters greater than 1.6 inches [7,9]. However, although the method could determine whether there was a flaw in CASS, the estimation of the precise size of the flaw was still inaccurate. Hence, there are no proven testing procedures and guidelines for assessing the degradation of CASS.

The research on UT for evaluating the thermal embrittlement of CASS has focused on accurately measuring the flaw size in a material as thermal embrittlement occurs; however, the measurement is difficult because of the high scattering and attenuation of the ultrasonic wave. Because of this problem, in this study, we do not measure the defect size to evaluate the thermal embrittlement of CASS but rather employ a different approach in which the changes in material properties are assessed for the thermal embrittlement evaluation. The changes in the material properties are assessed using a nonlinear ultrasonic technique (NUT), which is a potential nondestructive method [10]. For the assessment, we prepared thermally aged CF8M specimens; CF8M is one of the most sensitive materials to thermal embrittlement among different types of CASS. Nonlinear ultrasonic measurements were performed using a contact piezoelectric method to obtain the relative ultrasonic nonlinearity parameter, and a mini-sized tensile test was performed to investigate the correlation of the nonlinearity parameter with material properties.

2. Nonlinear ultrasonic technique

The NUT has been considered as a potential nondestructive evaluation method for assessing the early damage in a material. This technique is based on the nonlinear elastic interaction between a material and propagating ultrasonic wave. When the waveform of the incident monotonic ultrasonic wave is distorted during propagation in a material such that higher-order harmonic frequency components are generated, the amplitudes of the harmonic components are dependent on the elastic nonlinearity of the material. Thus, the NUT based on higher-order harmonic generation measures the amplitudes of the harmonic components after the propagation of the wave in a material to evaluate the level of elastic nonlinearity of the material. The nonlinearity parameter β is used to quantify the second-order nonlinearity, which is measured from the amplitude of the second-order harmonic frequency component [11]. It is well known that β is closely related to the microstructure of a material [12–16]. Kim et al. showed the dependence of nonlinear ultrasonic characteristics on the precipitation of a second phase in heat-treated Al6061-T6 [14]. Park et al. correlated the metallurgical properties and ultrasonic nonlinearity of 9–12Cr ferritic–martensitic steel [15]. Gutiérrez-Vargas et al. studied the characterization of thermal embrittlement in 2507 super duplex stainless due to spinodal decomposition of ferrite phase by measuring the ultrasonic nonlinearity [16]. Therefore, this nonlinearity parameter β can be used for evaluating the material degradation [12–16] caused by microstructural changes induced by degradation.

To measure the ultrasonic nonlinearity parameter β, the second-order harmonic detection method is used. That is, a finite-amplitude monotonic ultrasonic signal is transmitted into a material and then detected after propagation through it. The propagating ultrasonic wave undergoes distortion because of its nonlinear elastic interaction with the material, leading to the generation of the second-order harmonic component. Thus, the detected ultrasonic wave signals contain not only the fundamental excitation frequency but also its second-order harmonic frequency. The nonlinearity parameter β is determined from the displacement amplitudes of the fundamental and second-order harmonic frequency components as follows [11–28]:

$$\beta = \frac{8A_2}{A_1^2 k^2 x} \tag{1}$$

where A_1 and A_2 are the fundamental and second-order harmonic displacement amplitudes, respectively; k is the wavenumber of the fundamental frequency; and x is the propagation distance. Here, when k and x are constant, the nonlinearity parameter β can be replaced with the relative nonlinearity parameter β' as follows [11–28]:

$$\beta' = \frac{A_2'}{A_1'^2} \tag{2}$$

where A_1' and A_2' are the detected signal amplitudes of the fundamental and second-order harmonic components, respectively. Therefore, the relative nonlinearity parameter can be measured by using the voltage output signal detected by a piezoelectric transducer [11–28]. Note that while measuring the relative nonlinearity parameter, the measurement conditions such as the equipment type, measurement frequency, and specimen thickness should be kept constant. Although the relative nonlinearity parameter is different from the nonlinearity parameter, the former can be used for a relative comparison of nonlinearity before and after damage [28].

3. Specimens

We prepared five CF8M specimens with the same thickness of 10 mm. The chemical composition of the CF8M specimens is presented in Table 1. The specimens were obtained as annealed at 1050 °C for 4 h followed by water quenching [29]. Fig. 1 shows the scanning electron microscopy image of the as-received CF8M specimen. To perform the microscopy, the as-received specimen was etched in a solution of 20% sodium hydroxide (NaOH), and 80% dewater at a voltage of 3 V for 10 s. The as-received CF8M specimen contained irregularly dispersed δ-ferrite in an austenite matrix (Fig. 1) [29]. Then, other specimens were obtained by performing thermal aging under four different aging conditions (375 °C for 5000 h, 343 °C for 20000 h, 400 °C for 10000 h, and 400 °C for 20000 h). After the thermally aged specimens were prepared, nonlinear ultrasonic measurements were performed for each specimen; then, a mini-sized tensile test was performed using a mini-sized tensile specimen with a gage length of 5 mm, width of 1.2 mm, and thickness of 1 mm [29]. Then, the correlation of the nonlinearity parameter with the tensile properties (such as the tensile strength and elongation) was investigated because changes in the tensile strength and elongation are pronounced in thermally aged CF8M at temperatures between 300 °C and 450 °C [3,29].

4. Nonlinear ultrasonic measurements

Nonlinear ultrasonic measurements were performed using a

Table 1
Chemical composition of CF8M specimen.

Material	Fe	Cr	Ni	C	Si	Mn	Mo
Chemical Composition (%)	Bal.	22.05	10.22	0.058	0.80	0.83	2.14

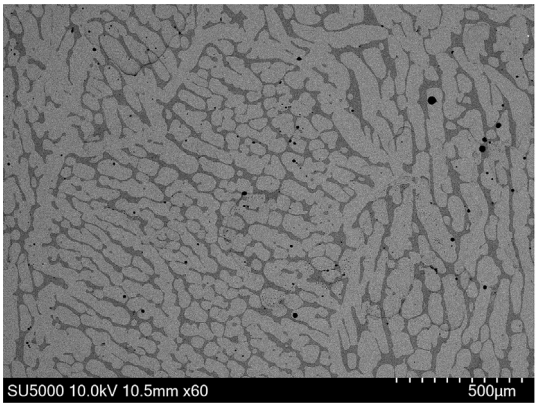

Fig. 1. Scanning electron microscopy image of as-received CF8M specimen.

through-transmission technique (Fig. 2). Generally, a low-frequency ultrasonic wave is transmitted to reduce the effect of attenuation on the assessment of the thermal embrittlement of CASS by flaw sizing. However, when low-frequency ultrasonic waves are generated, it is difficult to receive tone-burst ultrasonic wave signals that would facilitate the formation of a narrow bandwidth frequency spectrum for distinguishing between a fundamental frequency component and second-order harmonic frequency component. Therefore, we transmitted a 2.5 MHz ultrasonic wave using a PZT transducer with a center frequency of 2.25 MHz. Nevertheless, the attenuation effect can be neglected because the thickness of the specimen is as small as 10 mm. An input tone-burst signal with six cycles was generated from a high-power gated amplifier (RITEC, RAM-5000 SNAP). This high-voltage signal was passed through a 3 MHz low-pass filter to suppress the high-frequency components generated within the high-power gated amplifier. A constant contact pressure of 0.4 MPa was applied to two transducers using a pneumatic device to minimize variations in the contact condition during repeated measurements. The signals were obtained by a digital oscilloscope (Lecroy, HDO4043A). Fig. 3(a) shows a received signal from the as-received CF8M specimen. More than 100 signals were averaged to improve the signal-to-noise ratio. The frequency spectrum of the averaged signal was calculated using a fast Fourier transform (FFT) after applying a Hanning window. Fig. 3(b) shows the frequency spectrum of the signal in Fig. 3(a) from the spectrum, the magnitudes of

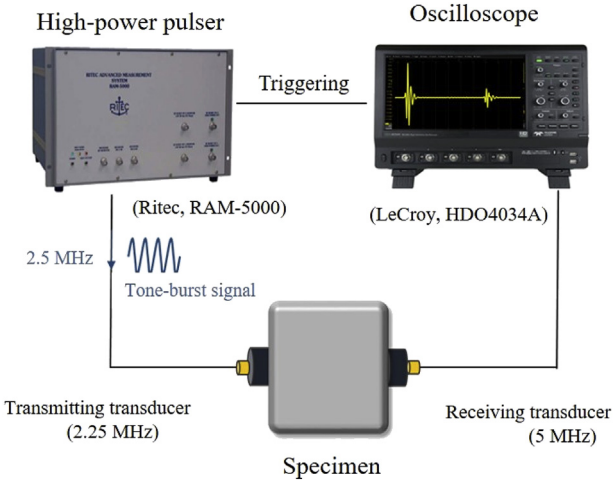

Fig. 2. Experimental setup for nonlinear ultrasonic measurement.

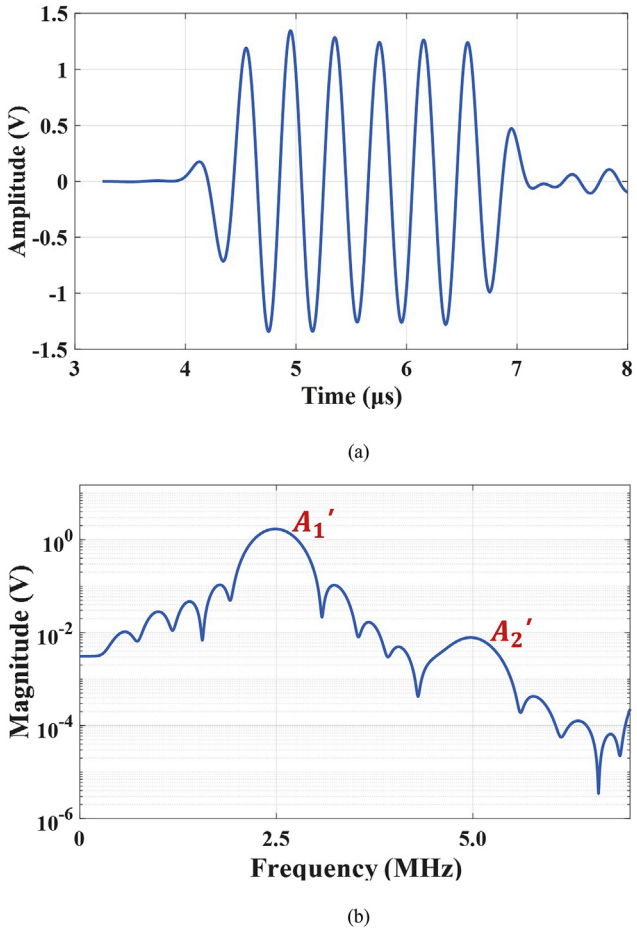

Fig. 3. (a) Received signal by oscilloscope and (b) FFT result of as-received CF8M.

the fundamental (A_1') and second-order harmonic frequency (A_2') components were determined. This process was repeated after increasing the input voltage levels to improve the reliability of measurement. Fig. 4 shows a good linear relationship (with a correlation coefficient of 0.99) between the square of the fundamental frequency component $A_1'^2$ and the amplitude of the second-order harmonic component A_2'. Finally, the relative nonlinearity parameter β' was determined by Eq. (2) using the slope of the fitted line ($A_1'^2$ vs. A_2').

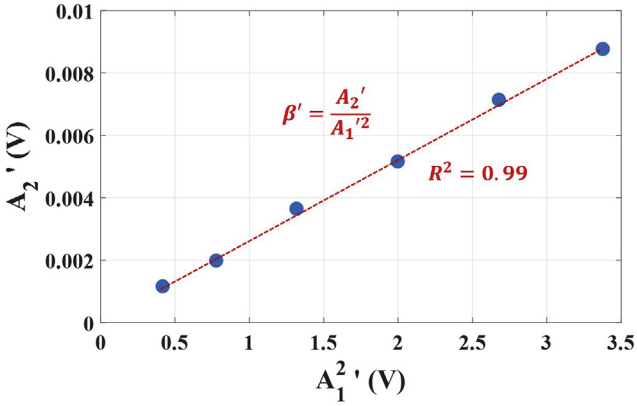

Fig. 4. Relationship between $A_1'^2$ and A_2' for as-received CF8M.

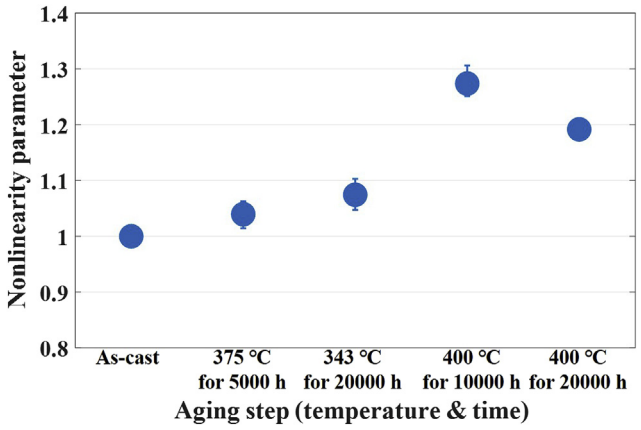

Fig. 5. Normalized relative ultrasonic nonlinearity parameter as function of aging steps.

5. Experimental results and discussion

Fig. 5 shows the relative ultrasonic nonlinearity parameter as a function of aging steps. The marked points are measured data and the error bar indicates the range of the maximum and minimum values (repeatability error is within 2%). The nonlinearity parameters are normalized by the value of the as-received specimen. The nonlinearity parameter value of the as-received specimen is different from those of the thermally aged specimens, and the difference is larger than the measurement variation. The nonlinearity parameter increases gradually and reaches its maximum value when the specimen is thermally aged at 400 °C for 10000 h. Fig. 6(a) shows the tensile strength and Fig. 6(b) shows the elongation as a function of the aging steps obtained from the mini-sized tensile test. As in the case of the nonlinearity parameter, the tensile strength also increases gradually and reaches its maximum value when the specimen is thermally aged at 400 °C for 10000 h. The variation in the tensile strength shows a close relationship with that in the nonlinearity parameter with the exponential regression correlation coefficient of 0.71. (Fig. 7 (a)). The increase in the tensile strength was attributed to spinodal decomposition in the ferrite phase, which is promotes the formation of two phase (Cr-rich and Fe-rich phases) that have the same crystal lattice type at the nanoscale [16,30,31], but different chemical composition and physical properties [16]. This spinodal decomposition may also affect the variation in the nonlinearity parameter. Therefore, the tensile strength and nonlinearity parameter behave similarly as a function of aging steps. The relationship between the nonlinearity parameter and spinodal decomposition should be further analyzed in the future.

The elongation, which decreases steadily, shows a different tendency with the nonlinearity parameter, which increases steadily, as a function of the aging steps. Nevertheless, the variations in the nonlinearity parameter and elongation show a close

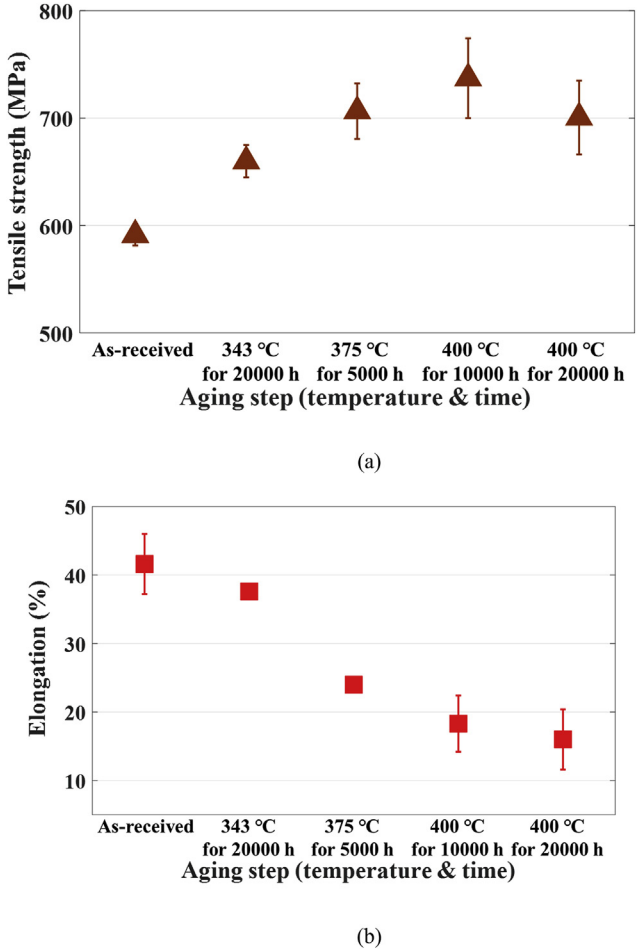

Fig. 6. Mini-sized tensile test results: (a) tensile strength and (b) elongation.

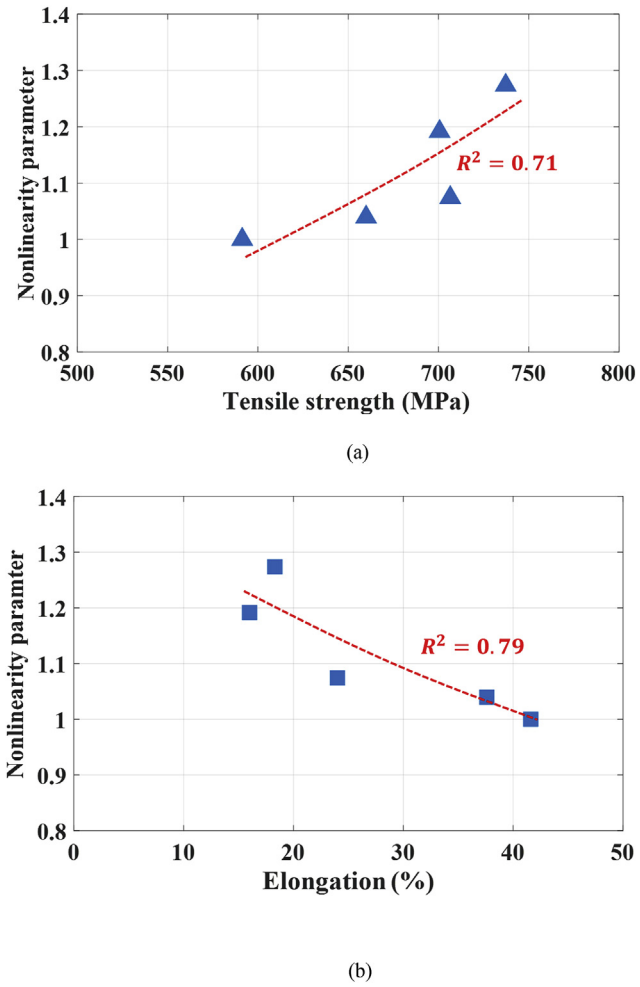

Fig. 7. Relationship between ultrasonic nonlinearity parameter and tensile properties: (a) tensile strength and (b) elongation.

relationship with the exponential regression correlation coefficient of 0.79 (Fig. 7(b)). Consequently, because the variation in the nonlinearity parameter is highly correlated with the variation in the material properties, the ultrasonic nonlinearity parameter can be used for assessing the thermal embrittlement of CASS.

6. Conclusion

In this study, we evaluated the thermal embrittlement of CASS using a NUT. We prepared CF8M specimens that were thermally aged under four different heating conditions. Nonlinear ultrasonic measurements were performed for each specimen followed by a mini-sized tensile test. The results show that the variation in the nonlinearity parameter is highly correlated with the variation in the tensile strength and elongation as a function of the aging steps. From the results of this feasibility study, we can confirm the applicability of the NUT to the evaluation of the thermal embrittlement of CASS used in PWRs.

Declarations of interest

None.

Acknowledgement

Funding: This research was supported by the Nuclear Safety Research Program of the Korea Foundation of Nuclear Safety (KoFONS) funded by the Nuclear Safety and Security Commission (NSSC) (No. 1805005) and by the Nuclear Power Research and Development Program of the National Research Foundation of Korea (NRF) funded by the Ministry of Science and Information & Communication Technology (ICT) (NRF-2017M2A8A4015158).

References

[1] O.K. Chopra, G. Ayrault, Aging Degradation of Cast Stainless Steel: Status and Program, Argonne National Labatory, CONF, 1983, pp. 8310143–8310165.
[2] O.K. Chopra, A. Sather, Initial Assessment of the Mechanisms and Significance of Low-Temperature Embrittlement of Cast Stainless Steels in LWR Systems, U. S. Nuclear Regulatory Commission & Argonne National Labatory, NUREG/CR-5385(ANL-89/17), 1990.
[3] U. S. Nuclear Regulatory Commission, Generic aging lessons learned (GALL) report, U. S. Nuclear Regulatory Commission, NUREG-1801, Rev 2 (2010).
[4] C.O. Ruud, A.A. Diaz, M.T. Anderson, Grain Structure Identification and Casting Parameters of Austenitic Stainless Steel (CASS) Piping, Pacific Northwest National Labatory, PNNL-19002, 2009.
[5] K. Sakamoto, T. Furukawa, I. Komura, Y. Kamiyama, T. Mihara, Study on the ultrasound propagation in cast austenitic stainless steel, E-J. Adv. Mainten. 4 (2012) 1–21.
[6] K. Sakamoto, T. Furukawa, I. Komura, Y. Kamiyama, T. Mih, Capability of ultrasonic testing for cast austenitic stainless steel in Japanese pressurized water reactors, E-J. Adv. Mainten. 4 (2012) 21–35.
[7] M.T. Anderson, S.L. Crawford, S.E. Cumblidge, K.M. Denslow, A.A. Diaz, S.R. Doctor, Assessment of Crack Detection in Heavy-Walled Cast Stainless Steel Piping Welds Using Advanced Low-Frequency Ultrasonic Methods, U. S. Nuclear Regulatory Commission & Pacific Northwest National Laboratory, NUREG/CR-6933(PNNL-16292), 2007.
[8] American Society of Mechanical Engineers, Rules for Inservice Inspection of Nuclear Power Plant Components, Section XI, ASME Boiler and Pressure Vessel Code, 2017.
[9] R.E. Jacob, T.L. Moran, A.E. Holmes, A.A. Diaz, M.S. Prowant, Interim Analysis of the EPRI CASS Round Robin Study, Pacific Northwest National Labatory, PNNL-27712, 2018, pp. 1–44.
[10] J. Kim, K.-Y. Jhang, Assessment of thermal degradation by cumulative variation of ultrasonic nonlinear parameter, Int. J. Precis. Eng. Manuf. 18 (2017) 23–29.
[11] K.-Y. Jhang, Application of nonlinear ultrasonics to the NDE of material degradation, IEEE Trans. Ultrason. Ferroelectr. Freq. Control 47 (2000) 540–548.
[12] K. Balasubramaniam, J.S. Valluri, R.V. Prakash, Creep damage characterization using a low amplitude nonlinear ultrasonic technique, Mater. Char. 62 (2011) 275–286.
[13] J. Kim, K.-Y. Jhang, Evaluation of ultrasonic conlinear characteristics in heat-treated aluminum alloy (Al-Mg-Si-Cu), Ann. Mater. Sci. Eng. 407846 (2013) 1–6.
[14] J. Kim, K.-Y. Jhang, C. Kim, Dependence of nonlinear ultrasonic characteristic on second-phase precipitation in heat-treated Al 6061-T6 alloy, Ultrasonics 82 (2018) 84–90.
[15] J. Park, M. Kim, B. Chi, C. Jang, Correlation of metallurgical analysis & higher harmonic ultrasound response for long term isothermally aged and crept FM steel for USC TPP turbine rotors, NDT Int. 54 (2013) 159–165.
[16] G. Gutiérrez-Vargas, A. Ruiz, J.-Y. Kim, L.J. Jacobs, Characterization of thermal embrittlement in 2507 super duplex stainless steel using nonlinear acoustic effects, NDT Int. 94 (2018) 101–108.
[17] M. Hong, Z. Su, Q. Wang, L. Cheng, X. Qing, Modeling nonlinearities of ultrasonic waves for fatigue damage characterization: theory, simulation, and experimental validation, Ultrasonics 54 (2014) 770–778.
[18] K.-Y. Jhang, Nonlinear ultrasonic techniques for nondestructive assessment of micro damage in material: a review, Int. J. Precis. Eng. Manuf. 10 (2009) 123–135.
[19] J.H. Cantrel, W.T. Yost, Effect of precipitate coherency strains on acoustic harmonic generation, J. Appl. Phys. 81 (1997) 2957–2962.
[20] J.H. Cantrell, Quantitative assessment of fatigue damage accumulation in wavy slip metals from acoustic harmonic generation, Philos. Mag. 86 (2006) 1539–1554.
[21] J.-Y. Kim, L.J. Jacobs, J. Qu, J.W. Littles, Experimental characterization of fatigue damage in a nickel-base superalloy using nonlinear ultrasonic waves, J. Acoust. Soc. Am. 120 (2006) 1266–1273.
[22] K.H. Matlack, J.-Y. Kim, L.J. Jacobs, J. Qu, Review of second harmonic generation measurement techniques for material state determination in metals, J. Nondestruct. Eval. 34 (2014) 273.
[23] A. Hikata, B.B. Chick, C. Elbaum, Dislocation contribution to the second harmonic generation of ultrasonic waves, J. Appl. Phys. 36 (1965) 229–236.
[24] C.-S. Seok, J.-P. Kim, Studies on the correlation between mechanical properties and ultrasonic parameters of aging lCr-lMo-0.25V steel, J. Mech. Sci. Technol. 19 (2005) 487–495.
[25] G.E. Dace, R.B. Thompson, O. Buck, Measurement of the acoustic harmonic generation for materials characterization using contact transducers, Rev. Prog. Quant. Nondestruct. Eval. 11B (1992) 2069–2076.
[26] A. Viswanath, B.P.C. Rao, S. Mahadevan, P. Parameswaran, T. Jayakumar, B. Raj, Nondestructive assessment of tensile properties of cold worked AISI type 304 stainless steel using nonlinear ultrasonic technique, J. Mater. Process. Technol. 211 (2011) 538–544.
[27] R.B. Thompson, O. Buck, D.O. Thompson, Higher harmonics of finite amplitude ultrasonic waves in solids, J. Acoust. Soc. Am. 59 (1976) 1087–1094.
[28] J. Kim, D.G. Song, K.Y. Jhang, A method to estimate the absolute ultrasonic nonlinearity parameter from relative measurements, Ultrasonics 77 (2017) 197–202.
[29] C. Jang, H. Jang, S. Hong, J.G. Lee, Evaluation of the recovery of thermal aging embrittlement of CF8M cast stainless steels after reversion heat treatments, Int. J. Press. Vessel. Pip. 131 (2015) 67–74.
[30] H. Jang, S. Hong, C. Jang, J.G. Lee, The effects of reversion heat treatment on the recovery of thermal aging embrittlement of CF8M cast stainless steels, Mater. Des. 56 (2014) 517–521.
[31] G.O. Subramanian, B.S. Kong, H.J. Lee, C. Jang, Evaluation of the thermal aging of δ-ferrite in austenitic stainless steel welds by electrochemical analysis, Sci. Rep. 8 (2018) 15091.